Biochemistry and Biophysics Reports 27 (2021) 101014

Contents lists available at ScienceDirect

Biochemistry and Biophysics Reports

journal homepage: www.elsevier.com/locate/bbrep

Two new sphingolipids from the stem bark of *Synsepalum msolo (Sapotaceae)*

Ache Roland Ndifor [a,*], Njinga Ngaitad Stanislaus [b], Chi Godloves Fru [c], Ferdinand Talontsi [d], Turibio Kuiate Tabopda [c], Elisabeth Zeuko'o Menkem [e], Ngadjui Bonaventure Tchaleu [c], Yeboah Samuel Owusu [f]

[a] *Higher Technical Teacher Training College, University of Bamenda, Cameroon*
[b] *Department of Pharmaceutical and Medicinal Chemistry, University of Ilorin, Ilorin, Nigeria*
[c] *Department of Organic Chemistry, Faculty of Science, University of Yaounde I, Cameroon*
[d] *Institute of Environmental Research (INFU), Faculty of Chemistry, TU Dortmund, Otto-Hahn-Str, 644221, Dortmund, Germany*
[e] *Department of Biochemistry, Faculty of Science, University of Yaounde I, Cameroon*
[f] *Department of Chemistry, University of Botswana, Gaborone, Botswana*

ARTICLE INFO

Keywords:
Sapotaceae
Synsepalum msolo
Phytoconstituents
Antibacterial
Antifungal

ABSTRACT

Synsepalum msolo commonly known as Bang Bali in Bali-Nguemba, Cameroon is used in traditional medicine against various diseases. The leaves and stem bark extracts were subjected to silica gel and Sephadex LH_{20} column chromatography to yield pure compounds. The structures of the compounds were determined by detail analysis of NMR and Mass spectroscopic data and by comparison with data reported in the literature. Amongst the isolates, were two new sphingolipids: synsepaloside B (**1**), synsepaloside C (**2**), and five known compounds: (+)-catechin (**3**), (−)-epicatechin (**4**), myricitrin (**5**), triacontanol (**6**), and aurantiamide acetate (**7**). Compounds **1**–**5** were screened for their antibacterial and anti-yeast activities on several microorganisms. All the tested compounds exhibited weak antibacterial (MIC $\geq$ 200 μg/mL) and anti-yeast (MIC > 200 μg/mL) activities as compared to standard: ciprofloxacin 0.468 < MIC >0.234 μg/mL and fluconazole MIC = 0.05 μg/mL, respectively.

1. Introduction

Medicinal plants provide major source of molecules with varying medicinal properties due to presence of natural compounds. These plants are useful for curing human diseases and play a vital role in healing due to presence of phytochemical constituents [1]. Cameroon has a very rich flora of medicinal plants serving as phytomedicine, amongst which *Synsepalum msolo* belonging to the family Sapotaceae and locally known as "Bang Bali'' in Bali of the North West region. The plant is found also in Bertoua and Nanga Eboko in the East region and in the East and tropical regions of Africa in Tanzania, Uganda, Kenya, Gabon, D.R. Congo, Ivory Coast and Ghana [2]. In Cameroon, the stem bark and roots are used to treat fever, headache, stomach ache and malaria [3]. The decoction of the dried stem bark of *Synsepalum msolo* alone or in combination with sugarcane is taken orally as a galactogogue in Tanzania [4,5]. In Taiwan the dried roots decoction is taken orally to treat diabetes mellitus [6]. Nonetheless, many plant species contain active ingredients such as alkaloids, phenols, tannins, cryogenics, glycocides, and terpeniods. These ingredients are used and found effective as sweeteners, anti-infections and anti-bacterials [7]. For instance, the stem bark, roots and leaves of *Synsepalum msolo* contain terpenoids (taraxeryl acetate, taraxerol, herranone, and betulinic acid), steroids (spinaterol and spinasterol-3-O-β-D glucopyranoside) and phenols (catechin, epicatechin and myricitrin) reported in numerous studies to demonstrate anticancer, anti HIV, antibacterial, antimalarial, analgesic, anti-inflammatory, antioxidant, anti-viral, and anti-allergenic activities [8–19]. Other classes of compounds isolated from this plant includes, saponins (pachystelanosides A and B) and sphingolipid (pachysteloside A) [13a,b]. Sphingolipids from eukaryotes and higher plant species are shown to exhibit antiulcerogenic activity [20], antifungal, antitumor, immunomodulating, antiviral, antitumor, immunostimulatory [21,22]; antiplasmodial, antileismanial, cytotoxic [23], cell proliferation, apoptosis, fungal pathogenesis and antibacterial activities [24–27]. Therefore, sphingolipids could be considered as active ingredients with

* Corresponding author.
E-mail address: achendifor@yahoo.com (A.R. Ndifor).

https://doi.org/10.1016/j.bbrep.2021.101014
Received 4 December 2020; Received in revised form 28 April 2021; Accepted 2 May 2021
Available online 11 June 2021

variant structures that might have potential therapeutic activities. In continuation of our investigation on *Synsepalum msolo*, we report herein the elucidation of the structures of two new sphingolipids and evaluation of their antibacterial and anti-yeast effects along with three known phenolic compounds on microorganisms.

2. Material and methods

2.1. Plant material

The leaves and stem bark of *Synsepalum msolo* were collected from Bali at "Manchung" in Southern Cameroon, in April 2013. Identification was done by Dr BathélémyTchiengue, a botanist of the Cameroon National Herberium, Yaounde, where voucher specimen (N° 3849/SRFK) was deposited.

2.2. General experimental procedure

All reagents were purchased from Merck, Darmstadt, Germany and are analytical grade. TLC was performed on silica gel 60 F_{254}, 0.1 mm thick (Merck) of size 20 × 20 cm. TLC spots were detected by fluorescence 254 nm or 366 nm and sprayed with 10% H_2SO_4 followed by heating at 70 °C. ^{1}H, ^{13}C, DEPT, COSY, HMQC, HSQC, HMBC spectra were recorded in deuterated solvent on either a Bruker Avance 600 MHz spectrometer or on Varian 500 MHz instrument. Chemical shifts are referenced to internal tetramethylsilane (δ = 0) and coupling constants *J* are reported in Hz. The Low-resolution electrospray-ionization mass spectrometry (ESI-MS) was carried out on a Micromass Quattro Micro mass spectrometer, HRTOFESI-MS and TOFESI-MS on micrOTOF 10237, Bruker compass Data Analysis 4.0. HRESI-MS data were obtained with an LTQ Orbitrap Spectrometer (Thermo Fisher, Waltham, MA, USA) equipped with an HESI-II source. IR spectra was recorded on a Perkin-Elmer spectrophotometer. Melting points were recorded using SMP3 melting point apparatus and is uncorrected.

2.3. Extraction and isolation

The powdered dry leaves (0.3 kg) and stem bark (3.3 kg) of *S. msolo* were extracted twice with CH_2Cl_2–CH_3OH (1:1 v/v) at ambient temperature for 2 days. The stem bark and leaves extract were concentrated under reduced pressure to yield dark brown viscous syrups (86 g) and black viscous syrup (100 g) respectively. 80 g of the stem bark extract was subjected to silica gel column and eluted with mixtures of n-hexane, ethyl acetate and methanol, in order of increasing polarities to give about 146 fractions. The similar fractions were combined using TLC analysis. Synsepaloside B **1** (6.4 mg), was directly obtained from fractions 121–124 (EtOAc-MeOH 20%) and synsepaloside C **2** (8.7 mg) from fractions 108–120. Aurantiamide acetate **7** (12 mg) and (−)-epicatechin **4** (30 mg) were directly obtained from fractions 82–87 and 100–106 respectively. 100 g of the leave extract was washed with n-hexane, ethyl acetate and methanol to yield 16 g, 18 g and 48 g respectively. The ethyl acetate fraction (18 g) was subjected over silica gel column and eluted with increasing polarity of n-hexane, ethyl acetate and methanol to give 124 fractions. The combination of similar fractions yielded triacontanol **6** (5 mg) and (+)-catechin **3** (6 mg). Fractions 121–124 from EtOAc-MeOH (80:20) was purified over Sephadex LH_{20} (100 MeOH) repeatedly to afford myricitrin **5** (19.2 mg). The compounds were identified using spectroscopic methods (1D and 2D NMR, MS).

2.3.1. Synsepaloside B (1)

White amorphous powder, mp 170.5 °C, $[\alpha]_D^{20}$+19.8 (*c* 0.1, MeOH); IR ν_{max} 3614, 3421, 2927, 1735, 1650, 1542, 1373, 1245, 1033 cm^{-1}; ^{1}H NMR (CD_3OD, 600 MHz) and ^{13}C NMR(CD_3OD, 150 MHz); HRESI-MS (positive-ion mode) at *m/z* 880.68431 $[M+H]^+$, (calcd for $C_{51}H_{93}NO_{10}$, 879.67995). ^{1}H-NMR (δ, 600 MHz): 5.44 (*m*, H-16), 5.43 (*m*, H-17, H-21, H-22), 5.39 (*m*, H-13), 5.37 (*m*, H-12), 5.36 (*m*, H-8), 5.35 (*m*, H-9), 4.32 (*d*, 7.8, H-1″), 4.28 (*d*, 4.8, 7.8, H-2), 4.07 (*dd*, 2.1, 10.5, H-1b), 4.05 (*d*, 6.0, H2′), 3.92 (*dd*, 3.9, 10.8, H-6a′′), 3.82 (*dd*, 3.6, 10.5, H-1a), 3.70 (dd, 3.9, 10.8, H-6b′′), 3.62 (*dd*, 6.0, 12.0, H-3), 3.54 (*dt*, 6.6, 12.6, H-4), 3.42 (*m*, H-5″), 3.38 (*m*, H-3″), 3.30 (*m*, H-4″), 3.20 (*dd*, 7.8, 8.7, H2″), 2.06 (*m*, H-10), 2.05 (*m*, H-5), 2.04 (*m*, H-7, H-11), 2.02 (*m*, H-6, H-15, H-18, H-21, H-24), 2.01 (*m*, H-3′), 2.00 (*m*, H-14, H-19, H-20, H-25), 1.70 (*m*, H-4′), 1.36 (*m*, H-5′), 1.30 (*s*, H-30), 1.28 (*br.s*, H-26 to H-27 and H-6′ to H-15′), 0.93(*t*, 6.6, H-29, H-16′). ^{13}C-NMR (δ, 150 MHz): 175.6 (C-1′), 130.2 (C-8, C-16, C-22), 130.0 (C-12, C-17), 129.5 (C-9, C-23), 129.4 (C-13), 103.4 (C-1″), 73.6 (C-2″), 76.6 (C-3″), 76.5 (C-5″), 74.1 (C-3), 71.6 (C-2′), 71.5 (C-4), 70.3 (C-4″), 68.5 (C-1), 61.3 (C-6″), 50.2 (C-2), 34.0 (C-5, C-11, C-18 C-24, C-3′), 32.3 (C-6), 32.0 (C-21), 31.6 (C-14, C-15, C-19, C-20, C-25), 29.2 (C-26 to C-27, C-4′ to C-14′), 26.6 (C-7, C-10), 22.4 (C-28, C-15′), 13.1 (C-29, C-16′), see Supplemental Table S1.

2.3.1.1. Methanolysis of synsepaloside B (1). Synsepaloside **B** (3.5 mg) was refluxed with 0.9 mol L^{-1} HCl in 82% aqueous MeOH (5 mL) for 20 h at a temperature of 60 °C. The resulting solution was extracted three times with n-hexane. The n-hexane solution was washed with water (5 mL) and dried over anhydrous Na_2SO_4 then concentrated to yield the fatty acid methyl ester (1.5 mg), identified as methyl hexadecanoate by analysis of GC-MS. Methyl hexadecanoate also known as hexadecanoic acid, 2-hydroxy- methylester was obtained as colorless oil, GC-MS: GC, t_R 17.416 min, *m/z* 286 (Cald. for $C_{17}H_{34}O_3$, 286.25), EI-MS: *m/z*: 227 [$M - C_{15}H_{31}O]^+$ (23), 71$[C_5H_{11}]^{+\cdot}$ (40), 57 $[C_4H_9]^{+\cdot}$ (90), see Supplemental Table S1 and supplementary data file.

2.3.2. Synsepaloside C (2)

White amorphous solid, mp 196.9 °C, $[\alpha]_D^{20}$ + 13.6 (*c* 0.1, MeOH); ^{1}H NMR (DMSO-d_6, 600 MHz) and ^{13}C NMR (DMSO-d_6, 150 MHz). HRTOFESI-MS (positive-ion mode), *m/z* 866.6593 $[M+Na]^+$, TOFESI-MS (positive-ion mode), *m/z* 866.7 $[M+Na]^+$, TOFESI-MS (negative-ion mode) *m/z* 842.7 $[M - H]^-$ (Cald. for $C_{48}H_{93}NO_{10}$, 843.6799). ^{1}H-NMR (δ, 600 MHz): 7.42 (*d*, 9.0, 2-NH), 5.38 (*dd*, 3.0, 13.2, H3′), 5.30 (*m*, H-4′), 4.90 (*d*, 3.9, 2″-OH), 4.71 (*s*, 3-OH), 4.47 (*t*, 5.7, 6″-OH), 4.28 (*d*, 5.7, 2′-OH), 4.14 (*d*, 7.8, H-1″), 4.09 (*m*, H-2), 3.87 (*m*, H-2′), 3.85 (*m*, H-5), 3.82 (*m*, H-1a), 3.66 (*m*, H-1b), 3.66 (*dd*, 6.0, 11.4, H-6″b), 3.45 (*dd*, 5.2, 11.4, H-6″a), 3.38 (*dd*, 8.1, 8.7, H-2″), 3.19 (*m*, H-5″), 3.16 (*m*, H-3″), 3.05 (*m*, H-4″), 2.94 (*dt*, 3.6, 8.4, H-3), 1.94 (*m*, H-5′), 1.76 (*m*, H-6), 1.24 (*br.s*, H-6 to H-15 and H-6′ to H-23′), 1.23 (*s*, H-16, H-24′) and 0.85 (*t*, 6.9, H-17, H-25′). ^{13}C-NMR (δ, 150 MHz): 173.7 (C-1′), 130.2 (C-3′), 129.8 (C-5′), 103.4 (C-1″), 74.0 (C-2″), 73.4 (C-3), 73.4 (C-3), 70.8 (C-4 and C-2′), 68.8 (C-1), 61.0 (C-6″), 49.8 (C-2), 31.8 (C-5′), 31.2 (C-5), 29.2 (C-6 to C-15; C-6′ to C-23′), 22.0 (C-16, C-24′) and 13.8 (C-17, C-25′), see Supplemental Table S2.

2.4. Preparation of stock solution

The stock solution of each compound, ciprofloxacin, and fluconazole were prepared in pure DMSO for a final concentration of 1 mg/mL. The stock solutions were filtered with a 0.20 μm sterilized syringe and stored at −20 °C until use.

2.5. Bacterial and yeast strains

Six bacterial strains: *Staphylococcus aureus* ATCC 43300, *Pseudomonas aeruginosa* NR48582, *Klebsiella pneumoneae* ATCC 700603, *Escherichia coli* ATCC 25922, *Shigella flexneri* NR518, *Streptococcus pneumoneae* HM145 and 3 yeast strains: *Candida albicans* NR 29445, *Candida albicans* NR 29451 and *Candida albicans* ATCC 29444 were assayed. Isolates were obtained from Yaounde Centre Hospital, Cameroon and the reference strains from BEI resources and the American Type Culture Collection Bacteria and yeast strains were cultivated

in petri dishes containing Muller Hinton Agar (MHA) and Sabouraud Dextrose Agar (SDA) respectively, followed by an incubation period of 24 h at 37 °C. Each microorganism was sub-cultured in a new Agar plate and incubated prior to each experiment.

2.6. Antimicrobial assays

The antimicrobial activity of each compound was assessed as recommended by the Clinical and Laboratory Standards Institute with minor modifications by the use of resazurin dye (CLSI, 2012) [28]. Briefly, forty μL of the compounds with concentration of 1 mg/mL was introduced in the microtiter plate containing 60 μL of culture medium for a final volume of 100 μL. 2-fold serial dilutions of samples were performedin 96-well microplates. The bacterial and yeast inoculum were prepared with sterile saline solution (NaCl 0.9%) using freshly cultured microorganisms of 24 h. Each suspension was adjusted to 0.5 McFarland standard then diluted in culture medium to yield a final concentration of 10^6 CFU/mL for bacteria and 1.5×10^3 CFU/mL for yeast. Fifty μL of each microbial suspension were added in each well and plates were incubated for 24 h at 37 °C. Thereafter, 10 μL of resazurin (0.15 mg/mL in PBS) was added followed by additional 4 h incubation and MIC was recorded visually as the lowest concentration of the compound required to inhibit 50% growth of pathogens. A negative control experiment was conducted using 0.1% DMSO.

3. Statistical analysis

All data were performed in triplicate and resulting MIC values expressed as mean ± standard deviation. The data were processed using the software SPSS 17.0 for Windows.

4. Results and discussion

Synsepaloside B (**1**) was isolated as white amorphous powder. Its molecular formula $C_{51}H_{93}NO_{10}$ was assigned on the basis of the HRESI-MS (positive-ion mode) at *m/z* 880.68431 $[M+H]^+$, and 1D and 2D NMR experiments. The IR spectrum showed absorption bands of hydroxyl (3341 cm^{-1}) and amide (1643 cm^{-1}) groups. The ^1H and ^{13}C NMR spectrum of **1** presented the characteristic signals of a *β*-D-glucopyranoside moiety (δ_H 4.11, 1H, *d*, $J = 7.8$ Hz, anomeric proton, δ_C 103.3 (CH), 70.2 (CH), 76.5 (CH), 76.6 (CH), 73.6 (CH), and 61.3 (CH_2)), an amide linkage 175.6 (C-1′), four olefinic methines δ_H 5.35 (1H, m, H-9), 5.36 (1H, m, H-8), 5.37 (1H, m, H-12), 5.39 (2H, m, H-13, H-23), 5.43 (2H, m, H-17, H-22), 5.44 (1H, m, H-16) with carbons at δ_C 129.4 (C-13), 129.5 (C-9, C-23), 130.2 (C-8, C-16, C-22), and 130.0 (C-12, C- 17), an amido methine (δ_H 4.28 (*d*, 4.8, 7.8, H-2), δ_C 50.2 (C-2)), an oxygenated methylene (δ_H 4.07 and δ_H 3.82; δ_C 68.5), three oxygenated methines (δ_H 3.62, 3.54, 4.05; and δ_C 74.1, 71.5, and 71.6), two terminal methyls (δ_H 0.93, 6H, t, $J = 6.6$ Hz) and two long aliphatic chains appearing as broad singlets (δ_H 1.28). Comparing these spectra data with literature studies indicates that compound **1** is a glycosphingolipid [29–31], (Fig. 1).

The methanolysis, of **1**, afforded fatty acid methylester, identified as hexadecanoic acid, 2-hydroxy- methylester and its molecular formula was established to be $C_{17}H_{34}O_3$ at *m/z* 286, in the GC-MS spectrum. See supplementary material.

In the HRESI-MS spectrum, the long-chain fatty acid (LCFA) [30] was determined to be 2-hydroxy-hexadecanoic acid due to the fragment ion at *m/z* 255 $[M - C_{16}H_{31}O_2] +$ (Fig. 2). The position of the 2-hydroxy group in the LCFA was confirmed by the α-cleavage of alcohol at *m/z* 227 $[C_{15}H_{31}O]^+$, in the HRESI-MS and GC-MS spectra (Fig. 2).

The long-chain base (LCB) [32] of compound **1** was derived as 2-amino-nonacosa-8,12,16,22-tetraen-1,3,4-triol by analysis of the ^1H–^1H COSY, HMQC and HRESI-MS, which showed a peak at *m/z* 463 $[M\text{-}163\text{-}255+2H]^+$. The ion peaks appearing at *m/z* 536 $[M - C_{25}H_{43}]^+$ and 476 $[M\text{-}C_{27}H_{47}O_2]^+$ indicated the presence of oxymethine carbons in LCB, assigned to positions C-3 and C-4 respectively, which were supported by the COSY correlations of H-1 through H-4 (Fig. 3). This was further supported by the ion peaks at *m/z* 532 $[M\text{-}18\text{-}C_{24}H_{41}]^+$, 476 $[M\text{-}C_{27}H_{45}O]^+$ and 337 $[M\text{-}2H_2O\text{-}163\text{-}343]^+$ resulting from Mc Lafferty rearrangement and the ^1H–^1H COSY correlations between the oxymethine δ_H 3.62 (dd, 6.0, 12.0 Hz, H-3) and δ_H 3.54 (dt, 6.6, 12.6 Hz, H-4), respectively (Figs. 2 and 3).

The positions of the olefinic double bonds at C-8/C-9 and C-12/C13 were affirmed by the ion peaks at *m/z* 301 $[C_{22}H_{37}]^+$, 275 $[C_{20}H_{35}]^+$, 221 $[C_{16}H_{29}]^+$, and 207 $[C_{16}H_{22}]^+$ in the positive ion mode HRESI-MS spectrum due to α/β-cleavages of the double bonds. In addition, the Mc Lafferty rearrangements resulting to the ion peaks at *m/z* 532 $[M\text{-}18\text{-}C_{24}H_{41}]^+$, 547 $[M\text{-}18\text{-}C_{23}H_{39}]^+$ and 451 $[M\text{-}18\text{-}C_{18}H_{31}]^+$ strongly confirmed the position of the double bonds at C8/C-9 and C-12/C-13, respectively (Fig. 2). The ion peak appearing at *m/z* 207 $[C_{15}H_{27}]^+$ and 153 $[C_{11}H_{21}]^+$ corroborate a third double bond at C-16/C-17 on the LCB. The peaks of the cleavages of an allylic bond at *m/z* 768 $[M - C_{18}H_{15}]^+$ and 794 $[M - C_6H_{13}]^+$ affirmed the fourth double bond position at C-22/C-23, on the LCB.

The *E* geometry at positions 12, 16 and 22 was supported by the chemical shift of the carbons next to the double bond at (δ_C 34.0 (C-11), δ_C 32.3 (C-14), δ_C 32.3 (C-15), δ_C 32.3 (C-18), δ_C 32.3 (C-21), δ_C 34.0 (C-24)), while the *Z* geometry at C-8/C-9 was affirmed by the chemical

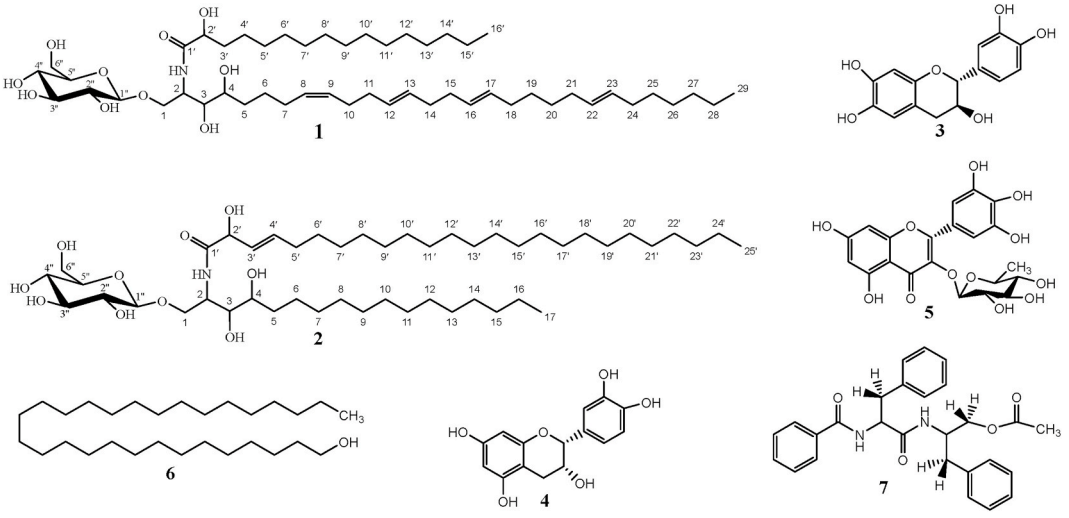

Fig. 1. Structure of isolated compounds.

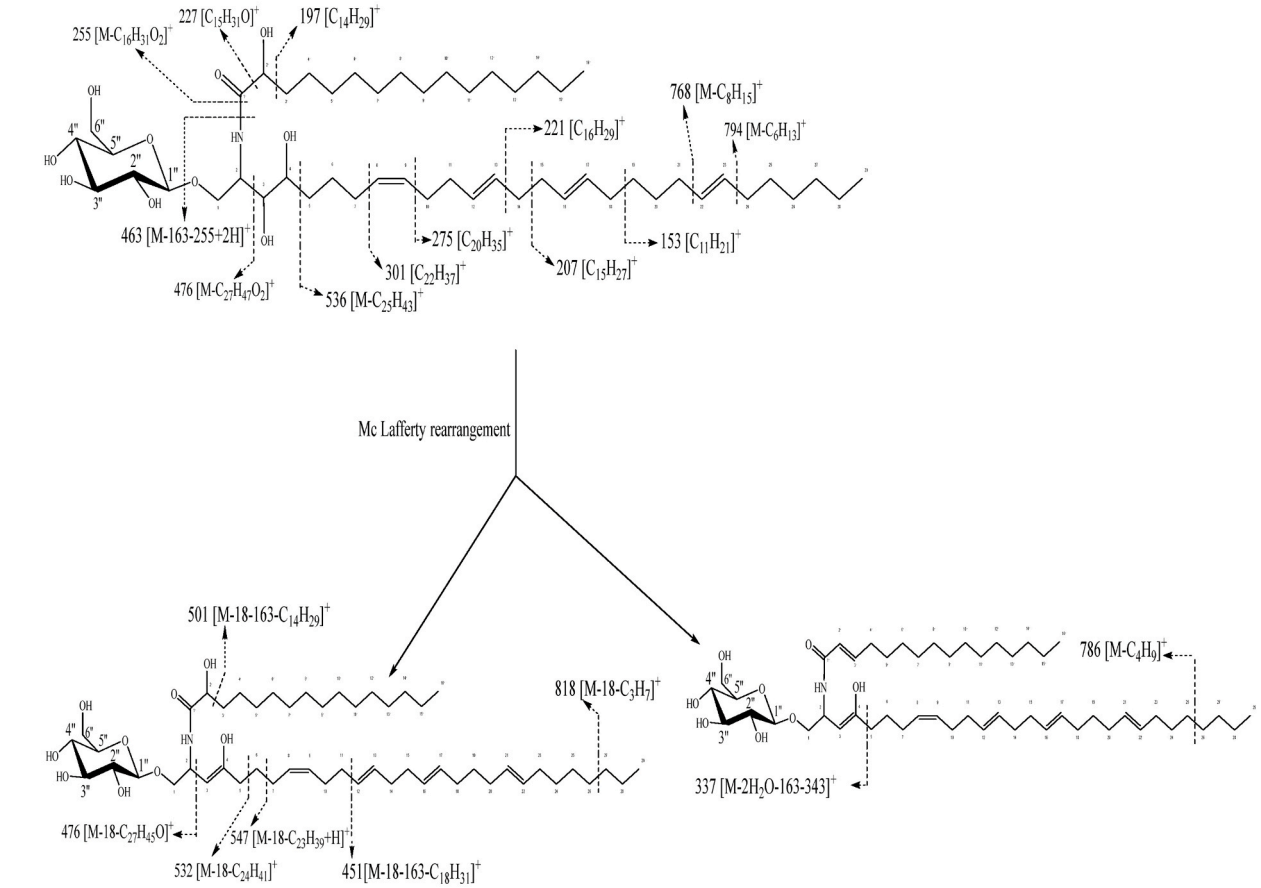

Fig. 2. Mass fragmentation pattern of synsepaloside B (**1**) following the HRESI-MS, GC-MS and ESI-MS.

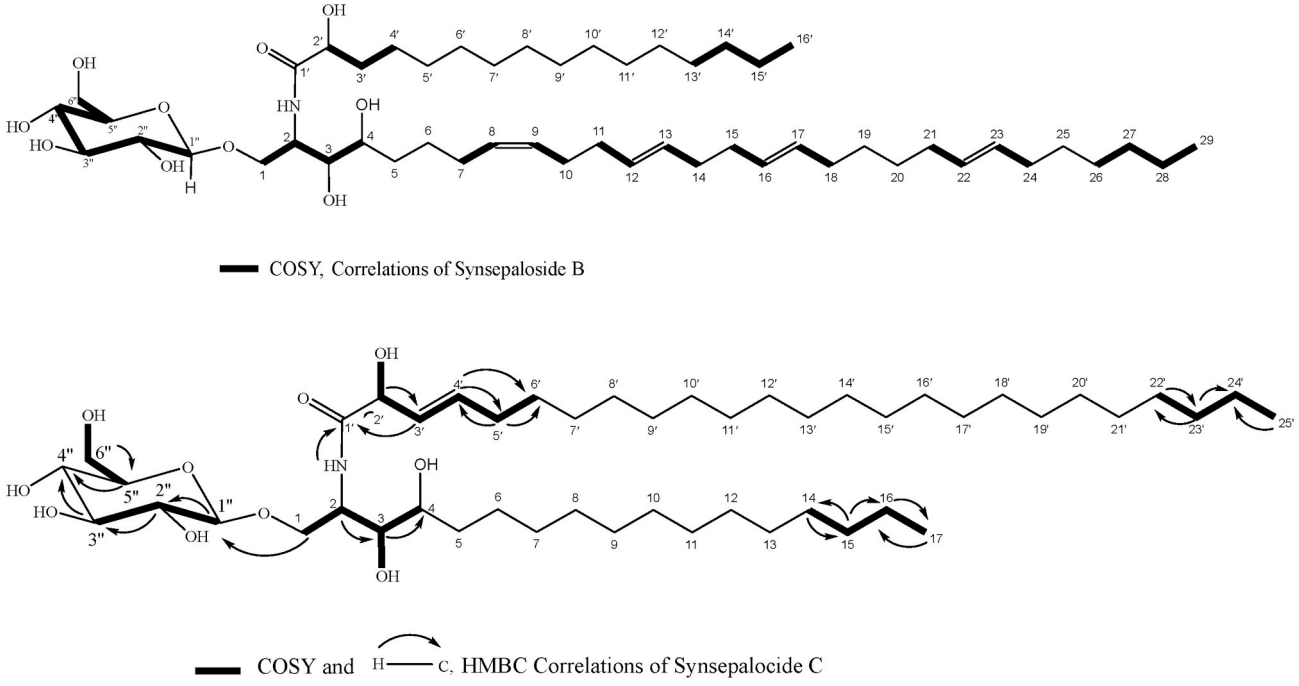

Fig. 3. Key COSY correlations of synsepaloside B (**1**). COSY and HMBC correlations of synsepaloside C (**2**).

shifts of the carbons next to the olefinic double bonds at (δ_C 26.6 (C-7) and δ_C 26.6 (C-10)). The chemical shifts for the adjacent carbons to a cis (*Z*) double bond appear in the range of δ_C 26–28 [33], while those of a trans (*E*) double bond appear in the range of δ_C 32–34 [30]. Thus, the Δ^8, was determined to be Cis (*Z*) due to the down field chemical shift values in the range of 26–28 [23], and Δ^{12}, Δ^{16} and Δ^{22} double bonds were

determined to be trans (*E*), due to their upfield chemical shift values in the range of 32–34 [29]. Therefore, the structure of compound **1** was determined as 1-*O*-*β*-D-glucopyranosyl-(8*Z*,12*E*,16*E*,22*E*)-2-[(2′)-2′-hydroxyhexadecanoylamino]-nonacosa-8,12,16,22-tetraen-1,3,4-triol, an unreported sphingolipid.

Synsepaloside C (**2**) was isolated as white amorphous solid. Its molecular formula $C_{48}H_{93}NO_{10}$ was deduced from its HRTOFESI-MS showing a pseudomolecular ion peak $[M+Na]^+$ at *m/z* 866.6593. The ^1H and ^{13}C NMR spectrum of **2** showed similar features to that of synsepaloside B. Compound **2** displayed resonances of a *β*-D-glucopyranoside moiety at (δ_H 4.15, 1H, *d*, *J* = 7.8 Hz, anomeric proton, δ_C 103.4 (CH), 70.0 (CH), 76.5 (CH), 76.9 (CH), 73.4 (CH), and 61.0 (CH_2)), an amide linkage (δ_H 7.42, 1H, *d*, *J* = 9.0 Hz, δ_C 173.7 (C-1′), an olefinic methine at δ_H 5.38 (*dd*, *J* = 3.0, 13.2 Hz, H-3′) and δ_H 5.30 (*m*, H-4′), assigned to carbon at δ_C 130.2 (C-3′) and δ_C 129.8 (C-4′), an oxygenated methylene (δ_H 3.66 and δ_H 3.82; δ_C 68.8), an amido methine (δ_H 4.09, *m*, H-2); δ_C 49.8), three oxygenated methines (δ_H 2.94, 3.85, 3.87; and δ_C 73.4, 70.8, and 70.8), two terminal methyls (δ_H 0.87, 6H, t, *J* = 6.9 Hz) and two long aliphatic chains appearing as broad singlets (δ_H 1.24). The comparison of these spectra data with literature values suggest that compound **2** is a glycosphingolipid [29–31], (Fig. 1). Compound **2** differs from **1** in that, **2** have a very long-chain fatty acid (VLCFA) [32]. The VLCFA was determined to be 2′-hydroxypentacos-3-enoic acid due to the characteristic fragment ion at *m/z* 381.3 (Fig. 4).

The molecular ion peak at *m/z* 295 was attributed to the α-cleavage that supported the location of the olefinic double bond at H-3'/H4′ in the VLCFA (Fig. 4). Furthermore, the fragment ion at *m/z* 335.1 resulting from the Mc Lafferty fragmentation processes strongly supports the position of the double bond and hydroxy function at H-2' (Fig. 4**)**. The signal of the olefinic double bond was observed at proton δ_H 5.38 (*dd*, *J* = 3.0, 13.2 Hz, H-3′) and δ_H 5.30 (*m*, H-4′), attributed to carbon at δ_C 130.2 (C-3′) and δ_C 129.8 (C-4′) respectively, in the VLCFA. The Δ^3 double bond of **2** was determined to be trans (*E*), by comparing the large vicinal coupling constant of the proton at δ_H 5.38 (1H, *dd*, *J* = 13.2 Hz, H-3′) and upfield chemical shift value of C-5′ in the range of 31.8, with literature data of flavuside B [27]. The LCB of **2** was determined to be 2-aminoheptadecan-1,3,4-triol due to fragment ion at *m/z* 301.2 (Fig. 4). The ion peaks at *m/z* 183 and 169 were attributed to the α/β-cleavages that confirmed the location of hydroxyl functions on the LCB. This was further supported by the COSY correlations for H-1 through H-5 (Fig. 3).

The connections through C1–O–C1″ and C2–NH–C1′ in compound **2** were strengthened using HMBC connectivity from H-2 to C-1 and C-3; from 2-NH to C-1'; from H-3 to C-4; from H-2′ to C-1'; from H-3′ to C-1′ and C-2'; from H-4′ to C-1′, C-5′ and C-6'; from 2′-OH to C-2'; from 3-OH to C-3 and C-4; from H-1 to C-1″, respectively. Therefore, the structure of **2** was established as 1-*O*-*β*-D-glucopyranosyl-2-[(2′,3′*E*)-2′-hydroxypentacos-3′-enoylamino]-heptadecan-1,3,4-triol, reported for the first time (Fig. 1).

Compounds **1**–**5**, were screened for their antibacterial and anti-yeast potency against 6 bacterial strains including *Staphylococcus aureus* ATCC 43300, *Pseudomonas aeruginosa* NR48582, *Klebsiella pneumoneae* ATCC 700603, *Escherichia coli* ATCC 25922, *Shigella flexneri* NR518, *Streptococcus pneumoneae* HM145 and 3 yeast strains *Candida albicans* NR 29445 *Candida albicans* NR 29451 and *Candida albicans* ATCC 29444. See Supplementary Table S3.

All the tested phytoconstituents exhibited weak activity on the bacteria and yeast strains with minimum inhibitory concentration (MIC) ≥ 200 μg/mL. However, as compared to the reference drugs ciprofloxacin and fluconazole, the tested products where much less active. These data suggest that the tested sphingolipids and phenolics of *Synsepalum msolo* were almost inactive in this experiment against the evaluated

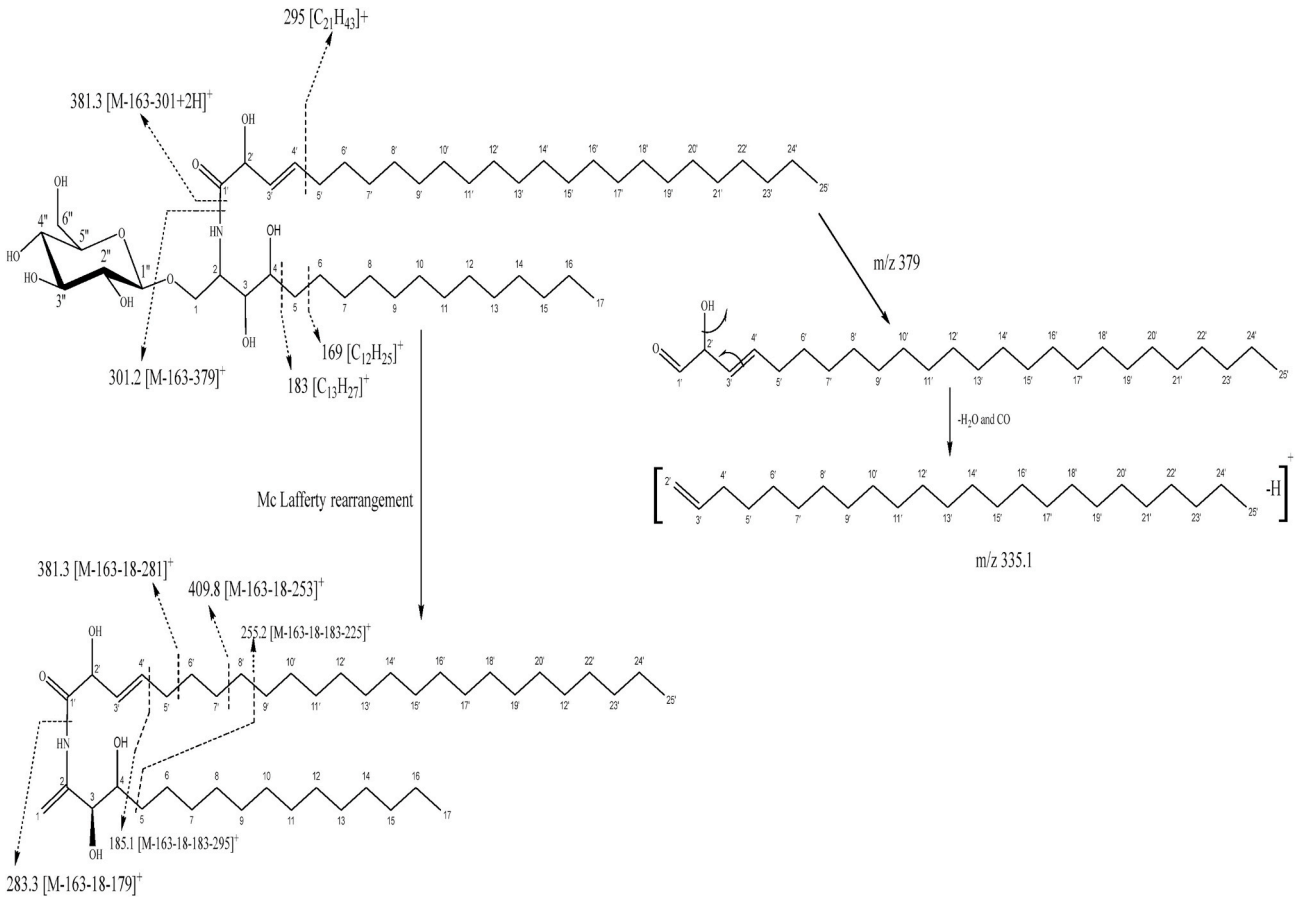

Fig. 4. TOFESI-MS mass fragmentation pattern of synsepaloside C (**2**).

microorganisms.

5. Conclusion

Two new sphingolipids [synsepaloside B (1) and synsepaloside C (2)], three phenolics [catechin (3), epicatechin (4) and myricitrin (5)], a fatty alcohol [triacontanol] and a peptide derivative [aurantiamide acetate] were isolated from the leaves and stem bark of a folk medicine *Synsepalum msolo*. Compounds **3**–**7** have known biological activities, and have not been reported previously as constituents of *Synsepalum msolo*. Analysis of the new sphingolipids and known compounds were done using NMR and mass spectra data and by comparison to those publish in the literature. The screening of the sphingolipids, catechin, epicatechin and myricitrin with several microorganisms demonstrated weak antibacterial and antifungal action. However, based on the weak activity observed, we recommend that other classes of compounds isolated from this plant in the future, should be subjected for investigations to identify the components with potent antibacterial and antifungal action.

CRediT authorship contribution statement

Ache Roland Ndifor: Conceptualization, methodology, data curation, investigation, writing original draft. **Njinga Ngaitad Stanislaus:** Data curation, writing original draft. **Chi Godloves Fru:** Data curation, writing original draft. **Ferdinand Talontsi:** Data curation, writing original draft. **Turibio Kuiate Tabopda:** Co-Supervision, project administration, data curation, writing original draft. **Elisabeth Zeuko'o Menkem:** Data curation, writing of original draft. **Ngadjui Bonaventure Tchaleu:** Supervision, project administration, funding acquisition. **Yeboah Samuel Owusu:** Project administration, funding acquisition, Investigation.

Declaration of competing interest

None.

Acknowledgements

The authors acknowledge the contributions of Dr Tala Michel Feussi and Dr Nana Federick for the accurate mass measurements. This work was partially funded by the Network for Analytical and Bio-assay Services in Africa (NABSA). Professor Fabrice Fekam Boyom Head of AntiMicrobial and Biocontrol Agents Unit focusing on Drug discovery against pathogenic protozoa, fungi, and bacteria, in the department of Biochemistry Faculty of Science, University of Yaounde I, Cameroon is acknowledged for performing the biological activity.

Appendix A. Supplementary data

Supplementary data to this article can be found online at https://doi.org/10.1016/j.bbrep.2021.101014.

References

[1] A.K. Garg, M. Faheem, S. Singh, Role of medicinal plant in human health disease, Asian J. Plant Sci. Res. 11 (1) (2021) 19–21.
[2] A. Aubréville, Sapotaceae, second ed., Flore du Cameroun, 1964, pp. 86–87.
[3] R.N. Ache, B.A. Keugni, L.A. Fotio, T. Dimo, O.S. Yeboah, B.T. Ngadjui, Analgesic and anti-inflammatory activities of herranone, spinasterol and crude extract of Pachystela msolo in rat and mice, WJPB 2 (2) (2015), 09–15.
[4] C.K. Ruffo, A. Birnie, B. Tengnäs, Edible Wild Plants of Tanzania, Regional L and Management Unit/Sida Technical Handbook, 2002, pp. 634–635.
[5] W. D Newmark, Ecological Studies 155, Conserving Biodiversity in East African Forests: A Study of the Eastern Arch Mountains, 2002, pp. 42–43.
[6] A.R. Ivan, Medicinal Plants of the World. Chemical Constituents, Traditional and Modern Medicinal Uses, 2005, pp. 438–439.
[7] O. Akinyemi, S.O. Oyewole, K.A. Jimoh, Medicinal plants and sustainable human health: a review, Hortic. Int. J. 2 (4) (2018) 194–195.
[8] J.-F. Hong, Y.-F. Song, Z. Liu, Z.-C. Zheng, H.-J. Chen, S.-S. Wang, Anticancer activity of taraxerol acetate in human glioblastoma cells and a mouse xenograft model via induction of autophagy and apoptotic cell death, cell cycle arrest and inhibition of cell migration, Mol. Med. Rep. 13 (2016) 4541–4548.
[9] J. Liao, F. Wu, W. Lin, Z. Huang, Taraxerol exerts potent anticancer effects via induction of apoptosis and inhibition of Nf-kB signalling pathway in human middle ear epithelial cholesteatoma cells, Trop. J. Pharmaceut. Res. June 17 (6) (2018) 1011–1017.
[10] C. Chandramu, R.D. Manohar, D.G. Krupadanam, R.V. Dashavantha, Isolation, characterization and biological activity of betulinic acid and ursolic acid from Vitex negundo L, Phytother Res. 17 (2) (2003) 129–134.
[11] T.Y. Fujioka, R. E Kashiwada, L.M. Kilkuskie, L.M. Cosentino, J.B. Ballas, W. P Jiang, I.S. Janzen, K.H. Chen Lee, Anti-AIDS Agents, 11. Betulinic acid and platanic acid as anti-HIV principles from syzygium claviflorum, and the anti-HIV activity of structurally related triterpenoids, J. Nat. Prod. 57 (2) (1994) 243–247.
[12] S. Arora, G. Kumar, S. Meena, Gas chromatography-mass spectroscopy analysis of root of an economically important plant, cenchrus ciliaris L. From tar desert, Rajasthan (India), Asian J. Pharmaceut. Clin. Res. 10 (64) (2017).
[13] (a) K.T. Ache, F. Turibio, M.F. Talontsi, O.S. Tala, Yeboah, B.T. Ngadjui, Characterization of constituents from the roots of pachystela msolo engler (Sapotaceae), IJCPS 3 (6) (2015) 1431–1435;
(b) R.N. Ache, K.T. Turibio, O.S. Yeboah, B.T. Ngadjui, Two new triterpenoidal saponins from roots of pachystela msolo, NPC 10 (11) (2015) 1933–1936.
[14] J.N. Nyemb, A.T. Tchinda, E. Talla, E. B Nanga, D. T Ngoudjou, C. Henoumont, S. Laurent, J. Iqbal, J.T. Mbafor, Vitellaroside, A new cerebroside from Vitellaria paradoxa (Sapotaceae) and its bioactivities, Nat. Prod. Chem. Res. 6 (1) (2018) 1–9.
[15] J. Shay, H.A. Elbaz, I. Lee, S.P. Zielske, M.H. Malek, M. Hüttemann, Review article: molecular mechanisms and therapeutic effects of (−) epicatechin and other polyphenols in cancer, inflammation, diabetes, and neurodegeneration, Oxid. Med. Cell. Longevity (2015) 1–13. ID 181260.
[16] J. Bae, N. Kim, Y. Shin, S.-Y. Kim, Y.-J. Kim, Activity of catechins and their applications, Biomed. Dermatol. 4 (8) (2020) 1–10.
[17] P.W. Taylor, J.M.T. Hamilton-Miller, P.D. Stapleton, Antimicrobial properties of green tea catechins, Food Sci. Technol. Bull. 2 (2005) 71–81.
[18] A. Ricardo, M.C. EscandÓn, T. Héctor, Antibacterial effect of kaempherol and (-)-epicatechin on Helicobacter pylor, Eur. Food Res. Technol. 242 (2016) 1495–1502.
[19] A. Dorothy, H.Y. Okoth, N. Chena, A. Koorbanally, Antibacterial and antioxidant activities of flavonoids from Lannea alta (Engl.) Engl, Aanacardiaceae, Phytochemistry Letters 6 (3) (2013) 476–481.
[20] E. Okuyama, M. Yamazaki, The principles of Tetragonia tetragonoides having antiulcerogenic activity. II. Isolation and structure of cerebrosides, Chem. Pharm. Bull. 31 (1983) 2209–2219.
[21] P. Muralidhar, P. Radhika, N. Krishna, R.D. Venkata, R.C. Bheemasankara, Sphingolipids from marine organisms: a review, Nat. Prod. Sci. 9 (2003) 117–142.
[22] C.R. Emura, T. Higuchi, Miyamoto, A.-F. Amphimelibiosides, Six new ceramide dihexosides isolated from a Japanese marine sponge amphimedon sp, J. Org. Chem. 70 (2005) 3031–3038.
[23] M.A. Tantry, A. Idris, I.A. Khan, Glycosylsphingolipids from euonymus japonicus thunb, Fitoterapia 89 (2013) 58–67.
[24] L.M. Obeid, C.M. Linardic, L.A. Karolak, Y.A. Hannun, Programmed cell death induced by ceramide, Science 259 (1993) 1769–1771.
[25] J. Cheng, T.S. Park, L.C. Chio, A.S. Fischl, X.S. Ye, Induction of apoptosis by sphingoid long-chain bases in Aspergillus nidulans, Mol. Cell Biol. 23 (2003) 163–177.
[26] C.D.L. Luberto, E.A. Toffaletti, S.C. Wills, A. Tucker, J.R. Casadevall, Y.A. Perfect, Hannun, M. Del-Poeta, Roles for inositol-phosphoryl ceramide synthase 1 (IPC1) in pathogenesis of Cryptococcus neoformans, Genes Dev. 15 (2001) 201–212.
[27] Y. Gouhua, S. Louis, Y. Keumja, S.L. Alain, K. Gun-Do, D.C. Hong, S.K. Jung, H. Jongki, W.S. Byeng, Flavusides A and B, Antibacterial cerebrosides from the marine-derived fungus Aspergillus flavus, Chem. Pharm. Bull. 59 (2011) 1174–1177.
[28] Clinical and Laboratory Standards Institute, Methods for dilution of antimicrobial susceptibility tests for bacteria that grow aerobically; approved standard — ninth edition. CLSI document M07–A9. https://doi.org/10.4103/0976-237X.91790, 2012.
[29] Z. Duo, H.B.X. Chen, T. Kai, G. Jun-Ming, H. Xiang-Zhong, J. Zhi-Yong, Two new sphingolipids from the leaves of piper betle L, Molecules 18 (2013) 11241–11249.
[30] A.-Q. Jia, X. Yang, W.-X. Wang, Y.-H. Jia, Glycocerebroside bearing a novel long-chain base from Sagina japonica (Caryophyllaceae), Fitoterapia 81 (2010) 540–545.
[31] F. Cateni, J. Zilic, G. Falsone, G. Scialino, E. Banfi, New cerebrosides from Euphorbia peplis L.: antimicrobial activity evaluation, Bioorg. Med. Chem. Lett 13 (2003) 4345–4350.
[32] V.M. Louise, A.N. Johnathan, D.M. Diana, F.D. Jean, Plant sphingolipids: their importance in cellular organization and adaption, Biochim. Biophys. Acta 1861 (2016) 1329–1335.
[33] D. Tazoo, K. Krohn, H. Hussain, S.F. Kouam, E.Z. Dongo, Laportoside A and Laportomide A: A new cerebroside and a new ceramide from leaves of Laportea ovalifolia, Zeitschrift für Naturforschung, Naturforsh. 62b (2007) 1208–1212.